A Kinetic Theory Model for Type II Core Collapse Supernovae

Terrance Strother

Department of Physics and Astronomy and
National Superconducting Cyclotron Laboratory,
Michigan State University
East Lansing, MI 48842, USA
E-mail: strothe6@pa.msu.edu

Wolfgang Bauer[*]

Department of Physics and Astronomy and
National Superconducting Cyclotron Laboratory,
Michigan State University
East Lansing, MI 48842, USA
E-mail: bauer@pa.msu.edu

Motivated by the success of kinetic theory in the description of observables in intermediate and high energy heavy ion collisions, we use kinetic theory to model the dynamics of core collapse supernovae. The specific way that we employ kinetic theory to solve the relevant transport equations allows us to explicitly model the propagation of neutrinos and a full ensemble of nuclei and treat neutrino-matter interactions in a very general way. With these abilities, our preliminary calculations have observed dynamics that may prove to be an entirely new neutrino capture induced supernova explosion mechanism.

---

[*]Speaker.

1. Introduction

Despite the many advances hydrodynamic based calculations have made in the field of supernova science, a great deal more must be done before these simulations can be regarded as complete. A truly complete hydrodynamic simulation would in principle have to model the dynamics of multiple fluids with strongly time dependent viscosities to simulate the presence of a full ensemble of nuclei and neutrinos in the full six-dimensional phase space in a completely general way. No hydrodynamic simulation can do this yet. Since state-of-the-art hydrodynamic calculations already strain the capabilities of high performance supercomputers, there may be a long wait before more complex models that simulate the dynamics of hundreds of different species of nuclei and neutrinos in a general way in the full six-dimensional phase space. This motivates us to move away from the traditional hydrodynamic approach that we are familiar with and draw from other disciplines of physics in an attempt to circumvent this technological roadblock. It turns out that the field nuclear collision modeling is an ideal candidate for this purpose.

Intermediate and high energy nuclear collisions have been very accurately modeled by simulations that made use of transport theories based on a semiclassical implementation of kinetic theory [1, 2, 3]. Given the similarities between the requirements that must be satisfied by simulations of nuclear collisions and supernovae [4, 5, 6, 7], such as the ability to model particle production, shock wave formation, collective deflection, as well as the interplay between regular and chaotic collective dynamics, it is tempting to implement these types of kinetic theory based approaches to model the physics and astrophysics of supernova explosions. This is the aim of our work.

As discussed in our previous work [8], the full potential of our code will be realized when it is run large multiprocessor installations. Once it is fully parallelized, it will be capable of efficiently calculating all desired statistical distributions in the full three-dimensional coordinate space while propagating test particles in the full six-dimensional phase space. However, for debugging purposes, we also want to provide ways to test the implementation of our ideas on a single processor. The preliminary calculations discussed here were performed exactly for that purpose and were simulations of the collapse and early stages of the explosion of a non-rotating spherically symmetric core [9]. While test particles were still propagated in the full six-dimensional phase space, due to statistical limitations imposed by working on a single processor [8], we assumed that all statistical distributions were spherically symmetric. The algorithms employed to calculate the spherically symmetric statistical distributions are discussed in detail in our previous work [8]. Furthermore, our weak nuclear reaction network was only partially activated during these preliminary simulations and no strong nuclear reactions were modeled. Since our approach to modeling these reactions is entirely new, we have elected to implement and test them in stages. The rest of the weak and strong nuclear reaction networks will be activated and tested after the ongoing parallelization process is complete.

The output generated by this series of single processor test calculations is well understood and consistent with the physics included in the model thus far, however not all of the results were expected. The emergence of what may prove to be a new supernova explosion mechanism was observed in all test calculations. This potential new explosion mechanism is discussed in sections 6 and 7.

2. Equations of Motion

The one-body transport equation for the baryon phase space density $f_b(xp)$ is given by [10]

$$\frac{\partial f_b(xp)}{\partial t} + \frac{\Pi^i}{E_b^*(p)}\nabla_i^x f_b(xp) \; - \; \frac{\Pi^\mu}{E_b^*(p)}\nabla_i^x U_\mu(x)\nabla_p^i f_b(xp) + \frac{M_b^*}{E_b^*(p)}\nabla_i^x U_s \nabla_p^i f_b(xp)$$

$$= I_{bb}^b(xp) + I_{b\nu}^b(xp) \tag{2.1}$$

for the particular state b of the baryon. The left hand side of (1) describes the temporal changes in the baryon phase space density due to interactions due to the interactions of the nucleons with the mean field vector and scalar potentials U_μ and U_s. The two source terms on the right hand side of (2.1) are collision integrals that that represent the effects that correlations due to the two-body baryon-baryon and baryon-neutrino collisions have the baryon phase space density respectively. For any neutrino species, the transport equation simplifies to an equation of motion that contains only the streaming and baryon-neutrino collision terms since there are no mean field contributions and the possible effects of neutrino-neutrino collisions are neglected,

$$\frac{\partial f_\nu(xk)}{\partial t} + \frac{k \cdot \nabla^x}{E_\nu(k)}f_\nu(xk) = I_{b\nu}^\nu(xk) \tag{2.2}$$

We want to point our, however, that neutrino oscillations (vacuum and/or matter-induced) between different lepton flavors can be explicitly included. It is through the baryon-neutrino collisions that the baryon and neutrino phase space densities can affect one another and the transport equations are coupled by the source terms that represent these effects.

3. Test Particle Method

To numerically solve the coupled baryon and neutrino transport equations (2.1) and (2.2), the so-called test particle method is used [11]. Instead of fully discritizing the relevant six-dimensional phase space and calculating the phase space densities in each grid cell in every time step, the test particle method only follows the initially occupied phase space cells in time and represent them by a finite number of imaginary test particles. These imaginary test particles are propagated in a way that models the physical evolution of the phase space. They interact with one another via mean field one-body potentials and scatter with realistic cross sections.

The test particle approach was originally used to model individual intermediate and high energy nuclear collisions [11]. In that microscopic system, there were many more test particles than there were physical particles. If we wish to use the test particle approach to model a macroscopic system containing a very large number of physical particles, it is clearly impossible to have the number of test particles, N_{tp}, exceed the number of physical particles, N_{phys}. Computational limitations require in such cases that $N_{phys}/N_{tp} \gg 1$.

The test particle approach can still be applicable in cases where $N_{phys}/N_{tp} \gg 1$, so long as N_{tp} is sufficiently large to capture the gross dynamics of the macroscopic system's phase space. The ratio N_{phys}/N_{tp} effectively determines a scale cutoff of sorts below which details cannot be resolved. When N_{phys}/N_{tp} becomes sufficiently large, some truly microscopic phenomena become

impossible to directly simulate with test particles. Therefore it must be established that these unresolvable details do not impact the gross phase space dynamics and/or can be taken into account indirectly. This can be accomplished with convergence tests.

The test particle method formally approximates the phase space density with a sum over delta functions

$$f(\vec{r}, \vec{p}, t) = \sum_{i=0}^{N_{tp}} \delta^3(\vec{r} - \vec{r}_i(t)) \delta^3(\vec{p} - \vec{p}_i(t)) \tag{3.1}$$

Insertion of this approximation of the phase space density into the transport equations (2.1) and (2.2) yields simple semi-classical first-order linear differential equations of motion for the centroid coordinates of each test particle. The fact that the baryon and neutrino transport equations are solved in an identical fashion means that the treatment of neutrino dynamics is on equal footing with that of baryons. This is a significant advantage that the test particle approach has over traditional hydrodynamic models.

4. Matter Test Particles

Matter test particles are used to propagate a full ensemble of nuclei and free baryons. An exhaustive description of matter test particle properties can be found in our previous works [12, 13]. Here it suffices to say the following. Each matter test particle has its own set of nuclear properties and temperature. Initially the nuclear properties and temperature of each matter test particle is determined by the initial conditions of the progenitor [9]. At later times, a matter test particle temperature can be changed by thermal mixing and both its nuclear properties and temperatures can be changed by weak and strong nuclear reactions. In this way, we explicitly model the propagation of an entire ensemble of nuclei and the rapid evolution of the entire core's composition can be modeled in a thermodynamically consistent way. This is superior to the standard tracking of the abundances of free protons, neutrons, alpha particles, and a "representative heavy nucleus" employed by most hydrodynamic calculations. Nuclear structure effects significantly impact electron and neutrino capture rates [14], and many of these effects can be missed if one speaks of a "representative heavy nucleus" instead of an ensemble of nuclei. By contrast, in our approach we propagate ensembles of test particles and let each one independently represent an isotope, with the isotope composition being dynamically altered due to the weak interactions with leptons during the course of the simulation, which eliminates the need for the "representative heavy nucleus" approximation.

Matter test particles have acquired two new features since our last publication [12]. In addition to implicitly representing the number of electron required to render them charge neutral, they also can implicitly represent electron-positron pairs. They are also now sensitive to not only the pressure exerted by the electron gas, but also the pressures exerted by the gas of free nucleons and nuclei as well as the radiation and positron gases. The degeneracy of the electron gas is expected to generally prevent the former from significantly affecting the system's dynamics and the strong dominance of the electron pressure in the core prevents the latter from doing so. Nevertheless, they are included for completeness.

4.1 Matter Test Particle Equations

After the insertion of the delta function approximation of the baryon phase space density into equation (2.1), it is found that the centroid of each matter test particle is subject to three mean field forces: a gravitational force, a nucleonic force, and a force generated by the pressure exerted by the local matter and radiation gas. Matter test particles can also scatter with one another. The equations of motion for the centroid coordinates of the matter test particles are given by the following first order differential equations

$$\frac{d}{dt}\vec{p}_j = \vec{F}_{G,j} + \vec{F}_{nuc}(\vec{r}_j) + \vec{F}_{gas}(\vec{r}_j) + \vec{\mathscr{C}}(\vec{p}_j)$$

$$\frac{d}{dt}\vec{r}_j = \frac{\vec{p}_j}{\sqrt{m^2 + p_j^2/c^2}} \tag{4.1}$$

$$j = 1,\ldots,N$$

where $\vec{F}_{G,j}$ is the gravitational force acting on the jth matter test particle, $\vec{\mathscr{C}}(\vec{p}_j)$ symbolizes the effects that two-body collisions with other matter test particles have on the jth matter test particle's momentum, and N is the number of matter test particles used to model the core and is constant.

4.2 Matter Test Particle Interactions

Single processor simulations that assume that statistical distributions are spherically symmetric model gravitation with a modified Newtonian monopole algorithm discussed in our previous works [15]. The calculation of the mean field nucleonic force acting on a matter test particle is also discussed in our previous works [12]. The average force the matter and radiation gas pressure exerts on a matter test particle is easily shown by analogy with our previous treatment of the electron gas [12, 13] to be given by

$$\vec{F}_{gas} = -\frac{M_{tp}}{\rho}\vec{\nabla}P_{tot} \tag{4.2}$$

where M_{tp} is the matter test particle mass, ρ is the local mass density, and the total matter and radiation gas pressure $P_{tot} = P_{rad} + P_{nuc} + P_{e^-} + P_{e^+}$. The pressures exerted by the radiation gas and the gas of free nucleons and nuclei, P_{rad} and P_{nuc}, are readily calculable and the finite temperature pressure exerted by relativistic gases of electrons and positrons, P_{e^-} and P_{e^+}, are interpolated from tables. In addition to the forces that matter test particles indirectly exert on one another, they can scatter off other nearby matter test particles. The way we model test particle scattering is explained at length in out previous work [16]. Here we simply state that test particle scatterings are modeled relativistically and semi-classically in a way similar to those used in the simulation of heavy ion collisions [17].

5. Neutrino Test Particles

Unlike the net baryon number, the number of neutrino test particles is not constant. Neutrino test particles can be created and destroyed. The latter process can be induced by a weak interaction

or by a neutrino test particle escaping the core. The number of neutrino test particles therefore varies greatly at different times during the simulation. The only neutrino production mechanism included in our preliminary test calculations is electron capture by nuclei and free protons. It is clear how to include other neutrino production mechanisms into our model as well as how to model the presence of all flavors of neutrinos and anti-neutrinos, but we have elected to proceed incrementally when constructing the weak reaction network for this completely new model. Subroutines that model other neutrino production process such as weak decay and pair production have been written, but they will not be integrated into the code until the ongoing parallelization process is complete.

Since it is easy to demonstrate that neutrino flavor oscillations are strongly suppressed in the core [18], only the presence of electron neutrinos is simulated by our test calculations. Neutrino test particles are assumed to be massless, move at the speed of light, and subject to no mean-field-type forces. The only way they can interact with other test particles is through scattering with or being captured by matter test particles. Thus the propagation of neutrino test particles between weak reaction sites is quite simple. Merely multiplying the intermediate unit momentum vector of a neutrino test particle by the speed of light and propagation time determines its new location. No complicated numerical method of approximating the solutions to differential equations is required. This light speed propagation does put limits in on the time step size. To realistically model the propagation of neutrino test particles within the constraints of our coordinate space cells, the time step size should be no larger than 10^{-5} s.

5.1 Neutrino Test Particle Creation

Since we do not explicitly simulate the presence of electrons, we rely upon electron capture rate tables to model the production of test particles representing neutrinos produced via electron capture. Because our simulation models the propagation of a full ensemble of nuclei, electron capture rates are needed for many rare isotopes far from the valley of beta stability. Currently no table exists that can satisfy our input needs in this regard. Until more comprehensive electron capture rate tables become available, we must extrapolate existing tabulated rates to the drip lines. For preliminary test calculations, the widely available Fuller-Fowler-Newman (FFN) table [19] is used as the source for electron capture rates. We extrapolate the rates from the FFN table to the nuclei not included in their table that we include in our simulation, and then reduce all entries by an order of magnitude. Our motivation for doing this is as follows. More recent calculations of weak reaction rates using new shell models of the distribution of Gamow-Teller strength have resulted in an improved and often reduced estimate of its strength compared to those the FFN calculations yielded using extrapolations of the known experimental rates and a simple single-state representation of this resonance [20]. The difference is often an order of magnitude or more, so this table serves as a reasonable estimate of the rates. Once our test calculations are complete, we plan on utilizing the improved electron capture rates calculated by Juodagalvis et al. [21].

5.2 Neutrino Test Particle Propagation

Beam attenuation arguments are ideally suited for calculating neutrino-matter interaction probabilities for neutrinos represented by a neutrino test particle. The probability that the neutrinos

represented by a neutrino test particle that moves from location $\vec{x}_1$ to $\vec{x}_2$ is taken to be given by

$$P_{int} = 1 - \exp\left[-\int_{\vec{x}_1}^{\vec{x}_2} \sum_i \sigma_i(\vec{x}) n_i(\vec{x}) d\vec{x}\right] \tag{5.1}$$

where the sum over i runs over all of the interaction channels available to the neutrino test particle between $\vec{x}_1$ and $\vec{x}_2$, n_i is the local number density of the ith species of particle, electrons, free baryons, or nuclei, and σ_i is the average effective interaction cross section corresponding to the ith interaction channel. The n_i's are readily calculable and the σ_i's are interpolated from tables [22]. Once the interaction probability (5.1) is calculated, a simple Monte-Carlo algorithm determines if the neutrino test particle interacts with matter. Interaction channels are selected by constructing relative probabilities out of weighted average effective cross sections and using another simple Monte-Carlo algorithm to choose a channel. The significant appeal that this very general way of modeling neutrino-matter interactions is that it applicable everywhere in the core. This is a major advantage this kinematic model has over its hydrodynamic counterparts. Typical hydrodynamic treatments of neutrinos are sufficient only in the extremely short and long mean free path limits and are quite problematic at intermediate values [23, 24].

6. New Dynamics

All of our test simulations have observed new dynamics that may prove to be an entirely new neutrino capture induced supernova explosion mechanism. The early stages of the collapse calculated by our code unfold identically to the accepted picture of supernova collapse. Electron capture rates initially slowly increased as the collapse progressed and at later times rapidly increased and eventually led to rapid deleptonization of the inner core. Not long after the inner region of the core begins to rapidly deleptonize, an unexpected phenomenon is observed in each test calculation. It is always found that neutrino captures at intermediate radii inside the inner region of the core deposit a large amount of electrons in a narrow spherical shell centered about a radius of approximately 45-55 km. This radially localized accumulation of electrons alters the electron number density gradient in such a way that substantially increases the outward pressure exerted by the electron gas in the region just outside the radius at which the most electrons are produced. The resultant electron gas pressure profile generates an outward explosion of matter at radii of approximately 55 km. Matter inside this region always collapses inward and formed a proto-remnant. This accumulation of electrons produced by neutrino capture is most easily seen in a plot of the electron fraction distribution. In Fig. 1 we show a plot of the electron fractions in the spherical shells the core is divided into for the purpose of calculating statistical distributions. The distribution is generated after the outward explosion of matter is well underway, and the impact that localized production of electrons has on the electron fraction distribution is apparent. It is clear that the accumulation of electrons produced by neutrino capture manifests itself as a well defined spike in the electron fraction distribution. Results similar to this were produced by each of our test calculations. One may be surprised by the strong effect of neutrino capture and argue this channel be strongly blocked by the electron sea. However, one has to keep in mind that the matter density is still only on the order of 10^{-3} of nuclear matter density at 50 km from the center at this time in the collapse.
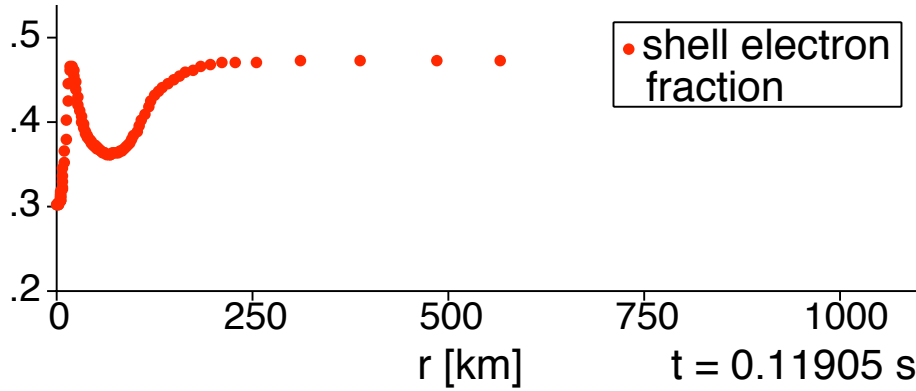
Figure 1: Plot of the electron fractions in the spherical shells after the outward explosion of matter is well underway.

7. Analysis of New Dynamics

This neutrino capture induces explosion mechanism substantially differs from the accepted bounce mechanism in many ways. The density in the region where the outward explosion of matter forms was always found to be on the order of 10^{-3} nuclear matter density while the central densities at that time were consistently found to be on the order of 0.1 nuclear matter density. This is a significant deviation from the accepted picture of bounce in which the initial outward explosion of matter is generated by the pressure exerted by matter at supernuclear densities accumulated in a small volume near the origin. Thus the role of the nuclear equation of state if fundamentally different in this scenario. Rather then directly dictating the how the outward explosion of matter is formed by determining the maximum density the central region can assume, it indirectly influences the neutrino capture induced explosion by governing the rate at which electron capture occur that power the explosion. The confluence of events that lead to the radial localization of the neutrino captures are well understood. An in depth discussion of them is beyond the scope of this article. Here it suffices to say that the origin of this phenomenon are rooted in weak reactions, nuclear structure effects and relativistic quantum electron gas statistical mechanics. Our ability to observe this phenomenon is critically dependent on our ability to propagate a full ensemble of nuclei and most importantly our ability to realistically model neutrino-matter interactions at intermediate densities.

8. Summary

We are encouraged by these preliminary results generated by our kinetic theory based model. The neutrino capture driven mechanism that it is uniquely poised to observe is robust enough to launch explosions in all test simulations conducted so far using three different nucleon potentials, four electron capture rate tables generated with the FFN table using different extrapolation techniques, and three different numbers of spherical shells used to calculate statistical distributions. However we realize that before we can contend that this picture is complete. In addition to completing the parallelization process and activating the three-dimensional subroutines, there is still more physics that needs to be added to our model. In particular fusion, several additional weak re-

actions, and the presence of excited nuclear states must all be built in. It is clear how to accomplish all of this with the test particle approach.

We are confident that this new explosion mechanism will survive the inclusion the aforementioned physics. The additional degrees of freedom introduced when three-dimensional distributions are calculated may destabilize the region in which electron are deposited by neutrino capture as it may be unstable to convection. An entropy analysis can confirm if this is a possibility. However even if convection does destabilize this region, the fact that convection begins at only ~ 1100 ms after the collapse begins at a radius on the order of 50 km would be a significant discovery in and of itself. The future of this model looks extremely bright and we look forward to continuing to advance it.

References

[1] G.F. Bertsch, H. Kruse, and S. Das Gupta, *Boltzmann equation for heavy ion collisions*, Phys. Rev. C **29** (1984) 673.

[2] H. Kruse, B.V. Jacak, and H. Stöcker, *Microscopic theory of pion production and sidewards flow in heavy-ion collisions*, Phys. Rev. Lett. **54** (1985) 289.

[3] W. Bauer, G.F. Bertsch, W. Gassing, and U. Mosel, *Energetic photons from intermediate energy proton- and heavy-ion-induced reactions*, Phys. Rev. C **34** (1986) 2127.

[4] J.R. Wilson, *Numerical astrophysics*, Jones and Bartlett, Boston, 1985.

[5] M. Herant, W. Benz, W.R. Hix, C.L. Fryer, and S.A. Colgate, *Inside the supernova: A powerful convective engine*, Astrophys. J. **435** (1994) 339.

[6] C.L. Fryer and A. Heger, *Core-collapse simulations of rotating stars*, Astrophys. J. **541** (2000) 1033.

[7] H.-T. Janka, K. Langanke, A. Marek, G. Martínez-Pinedo, and B. Müller, *Theory of core-collapse supernovae*, Phys. Rep. **442** (2007) 38.

[8] T. Strother and W. Bauer, *Modeling weak interaction rates during the supernova collapse phase*, Prog. Part. Nucl. Phys., **62** (2009) 468.

[9] S.E. Woosley and T.A. Weaver, *The physics of supernova explosions*, Ann. Rev. Astron. Astrophys. **24** (1986) 205.

[10] W. Bauer, *Dynamical simulations of supernovae collapse and nuclear collisions via the test particle method - similarities and differences*, Acta Phys. Hung. A **21** (2004) 371.

[11] C.-Y. Wong, *Dynamics of nuclear fluid. VIII. Time-dependent Hartree-Fock approximation from a classical point of view*, Phys. Rev. C **25** (1982) 1460.

[12] T. Strother and W. Bauer, *Neutrino capture induced supernova explosions*, submitted to *Int. J. Mod. Phys. D*.

[13] T. Strother, *A kinetic theory based numerical study of core collapse supernova dynamics*, Doctoral Dissertation, Michigan State University, 2009.

[14] G. Matrínez, M. Liebendörfer, and D. Frekers, *Nuclear input for core-collapse models*, Nucl. Phys. A, **777** (2006) 395.

[15] W. Bauer and T. Strother, *Collective motion in nuclear collisions and supernova explosions*, Int. J. Mod. Phys. E **14** (2005) 129.

[16] T. Strother and W. Bauer, *Nuclear physics and supernova explosions: Unified dynamics*, submitted to *Int. J. Mod. Phys. D*.

[17] G. Kortemeyer, F. Daffin, and W. Bauer, *Nuclear flow in consistent boltzmann algorithm models*, *Phys. Lett.* **B374** (1996) 25.

[18] L. Wolfenstein, *Neutrino oscillations in matter*, *Phys. Rev. D* **17** (1978) 2369.

[19] G. Fuller, W. Fowler, and M. Newman, *Stellar Weak Interaction Rates for Intermediate-Mass Nuclei IV. Interpolation Procedures for Rapidly Varying Lepton Capture Rates Using Effective* $\log(ft)$ *Values*, *Astrophys. J.*, **293** (1985) 1.

[20] A. Heger, S. E. Woosley, G. MartŠnez-Pinedo, and K. Langanke, *Presupernova evolution with improved rates for weak interactions*, *Astrophys. J.*, **560** (2001) 307.

[21] A. Juodagalvis, K. Langanke, W.R. Hix, G. Martinez-Pinedo, J.M. Sampaio, *Improved estimate of stellar electron capture rates on nuclei*: submitted to *Phys. Rev.* D

[22] A. Burrows and T. Thompson, *Neutrino-matter interaction rates in supernovae: The essential microphysics of core collapse*, to be published in *Core Collapse of Massive Stars*, ed. C. Fryer, Kluwer Academic Publishers.

[23] M. Herant, W. Benz, and S. Colgate, *Postcollapse Hydrodynamics of SN 1987A: Two-Dimensional Simulations of the Early Evolution*, *Astrophys. J.*, **395** (1992) 642.

[24] M. Herant, W. Benz, W. Hix, C. Fryer and S. Colgate, *Inside the Supernova: A Powerful Convective Engine*, *Astrophys. J.*, **435** (1994) 339.

PoS(BORMIO2010)022